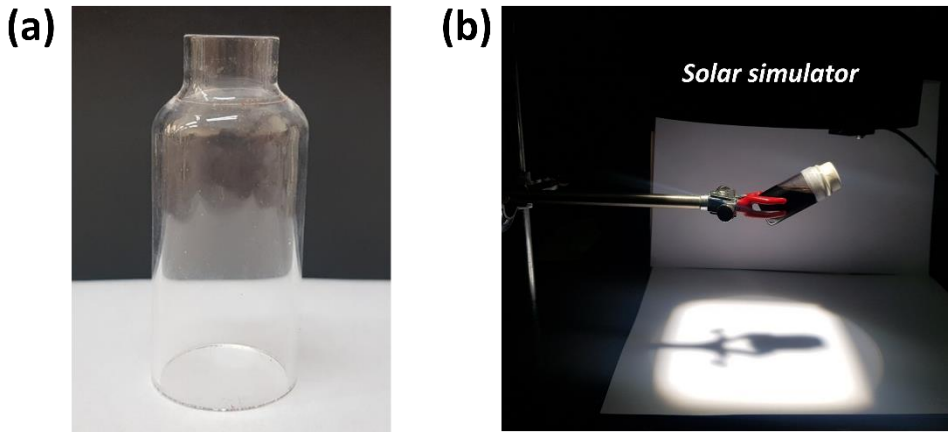

Supplementary Figure 1. Photograph of (a) lab-made quartz vial and (b) simulated sunlight irradiation in precursor solution of hcc-COF.

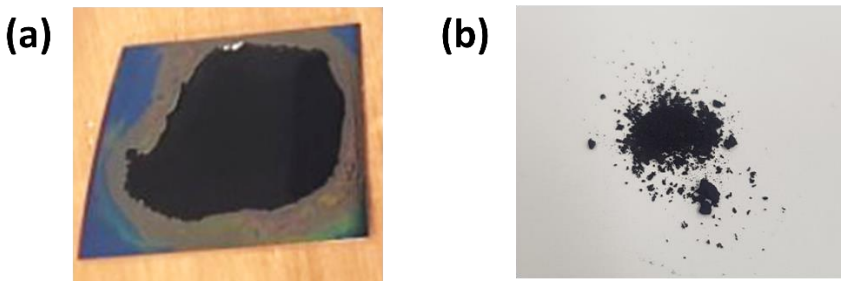

Supplementary Figure 2. Photograph of resulting hcc-COF (a) before and (b) after drying.

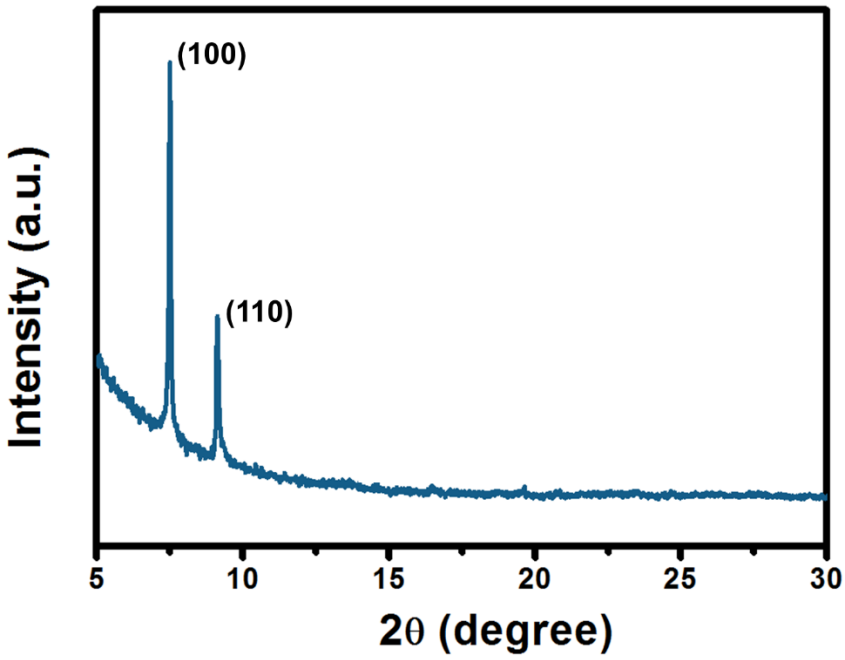

Supplementary Figure 3. PXRD spectra of the hcc-COF powder.

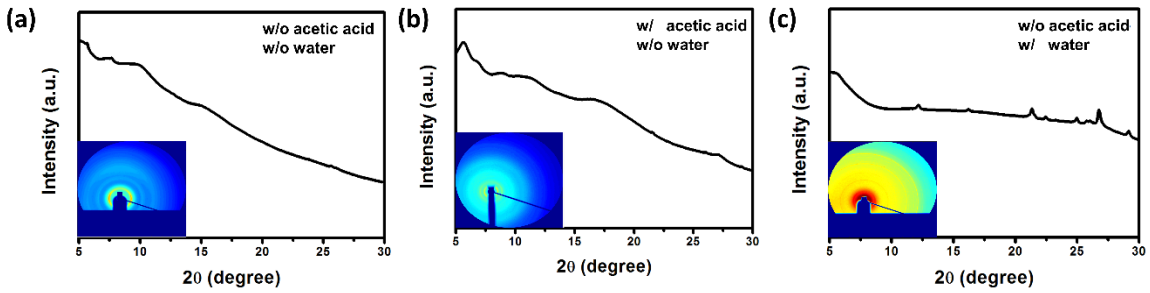

Supplementary Figure 4. WAXD patterns of resulting products obtained by different synthetic conditions: (a) without (w/o) addition of acetic acid and water (b) with (w/) acetic acid and w/o water (c) w/o addition of acetic acid and w/ water.

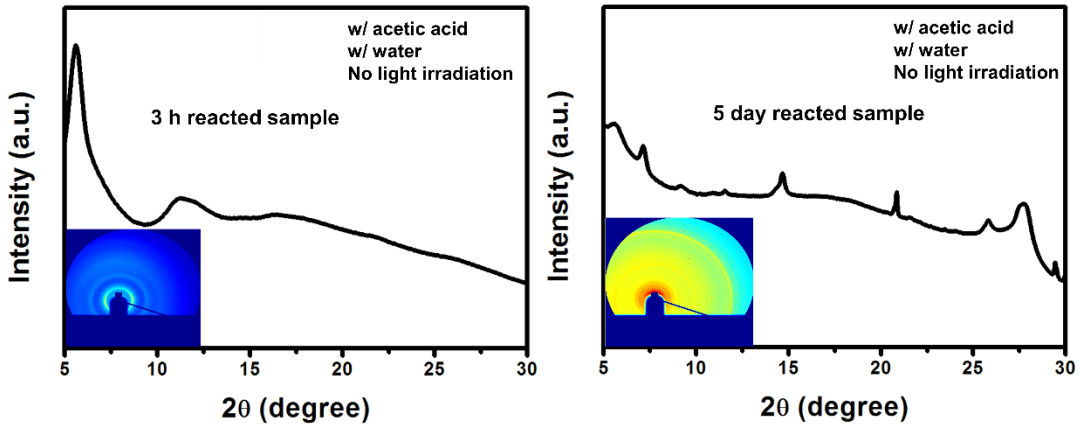

Supplementary Figure 5. WAXD patterns of resulting products obtained by different synthetic conditions: (a) 3 h and (b) 5 day reacted samples with no light irradiation under presence of acetic acid and water

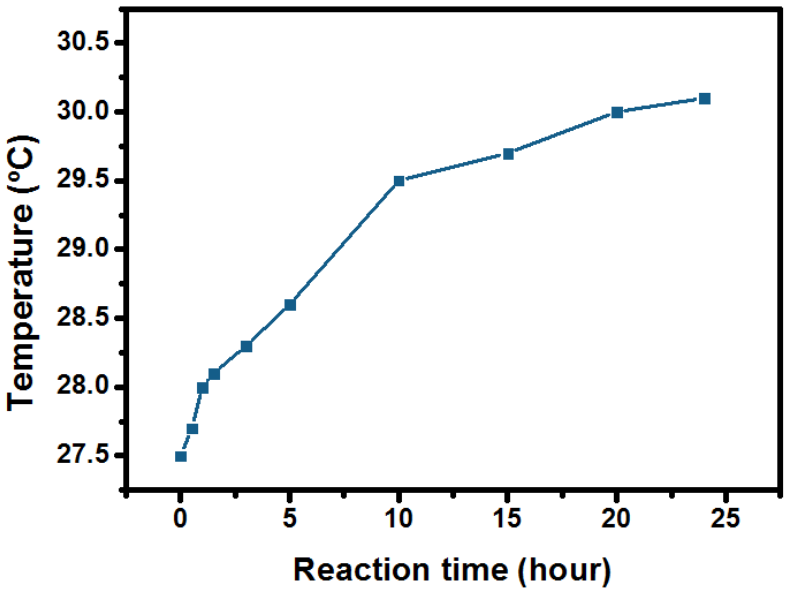

Supplementary Figure 6. The temperature changes of the reaction solution depending on the reaction time during the synthesis of the hcc-COF using solar simulator

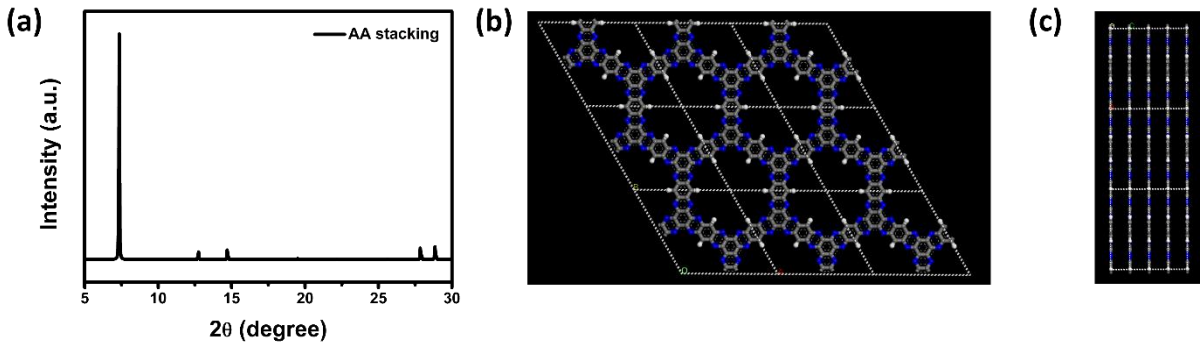

Supplementary Figure 7. (a) Calculated diffraction pattern, (b) top and (c) side view of optimized AA-stacked hcc-COF.

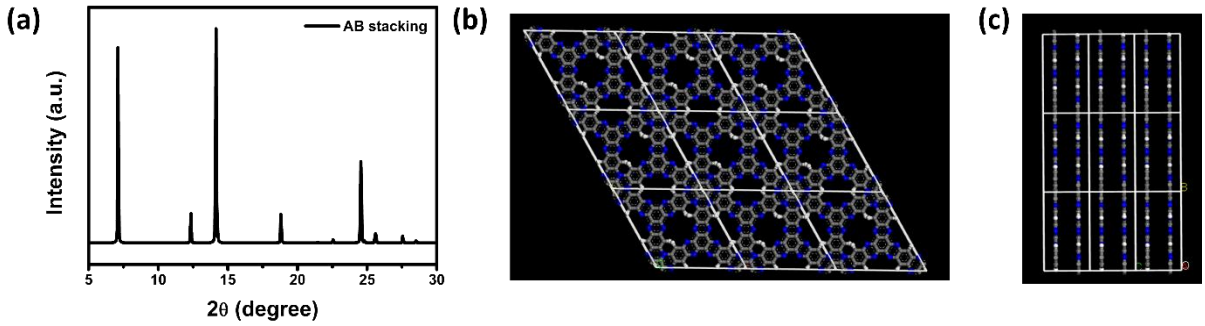

Supplementary Figure 8. (a) Calculated diffraction pattern, (b) top and (c) side view of optimized AB-stacked hcc-COF.

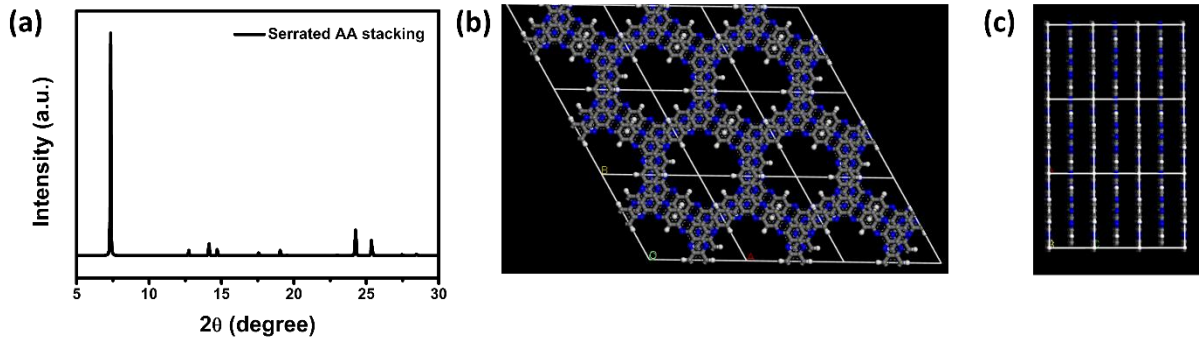

Supplementary Figure 9. (a) Calculated diffraction pattern, (b) top and (c) side view of optimized serrated AA-stacked hcc-COF.

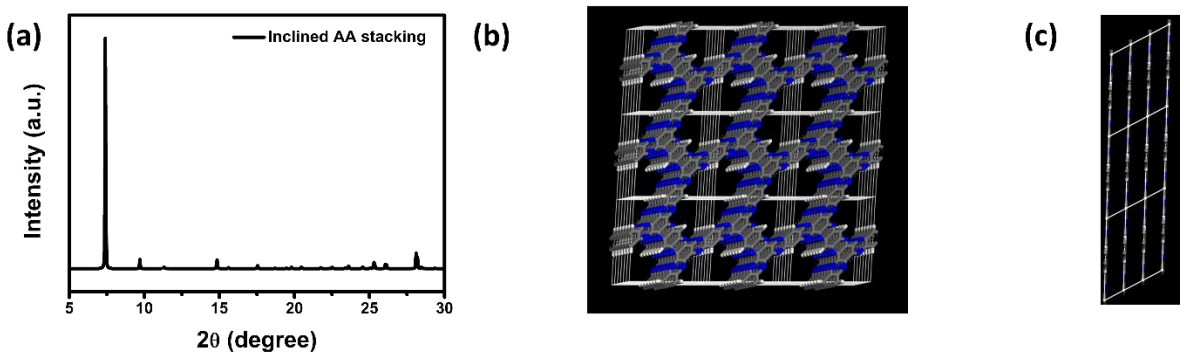

Supplementary Figure 10. (a) Calculated diffraction pattern, (b) top and (c) side view of optimized inclined AA-stacked hcc-COF.

(a)

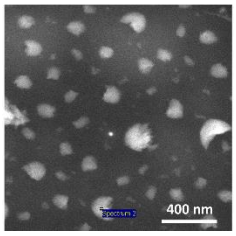

(b)

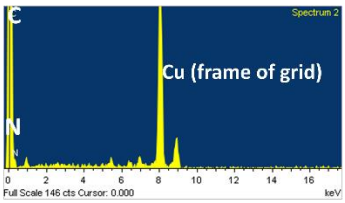

(c)

Element	Weight%	Atomic%
C K	73.52	76.40
N K	26.48	23.60
Totals	100.00	

Supplementary Figure 11. (a) Dark field TEM Image of hcc-COF for EDS mapping. (b) EDS mapping spectrum and (c) calculated elemental composition of hcc-COF

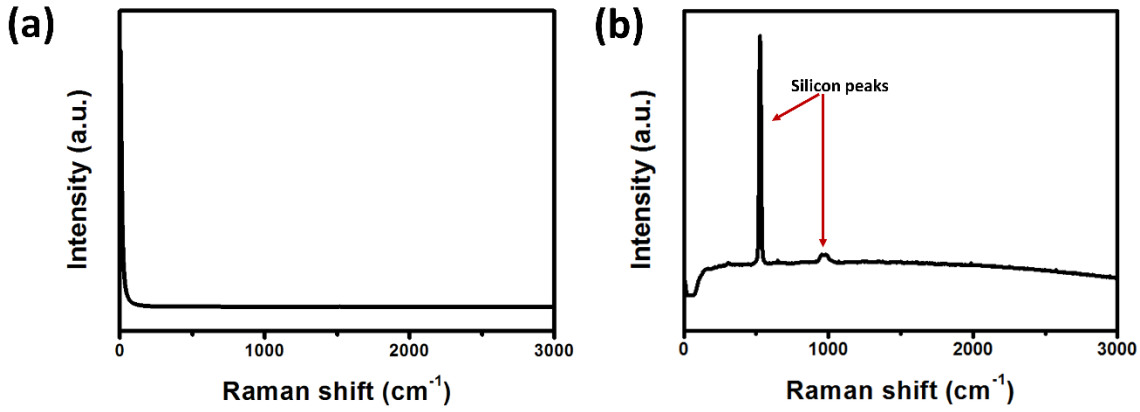

Supplementary Figure 12. (a) Calculated and (b) experimentally obtained Raman spectra of HCH precursor

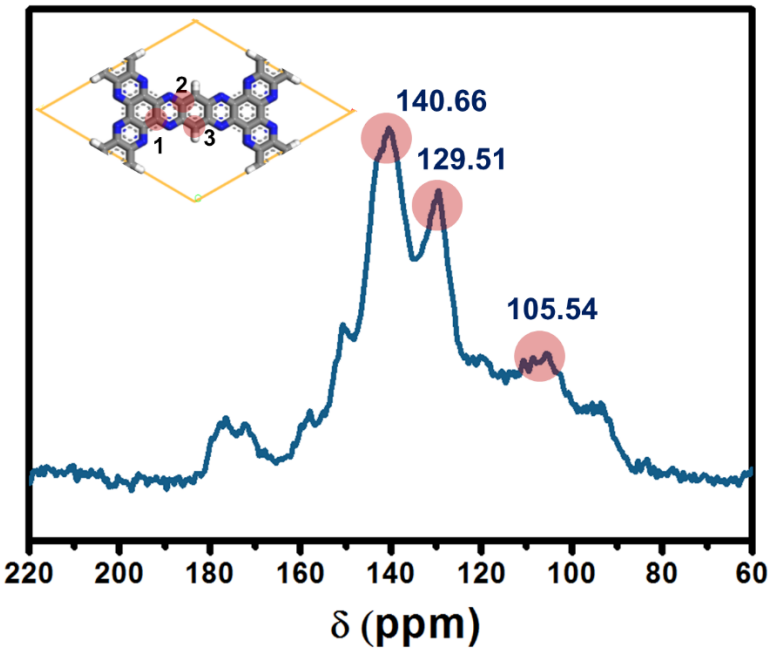

Supplementary Figure 13. ^{13}C solid NMR spectrum of the hcc-COF.

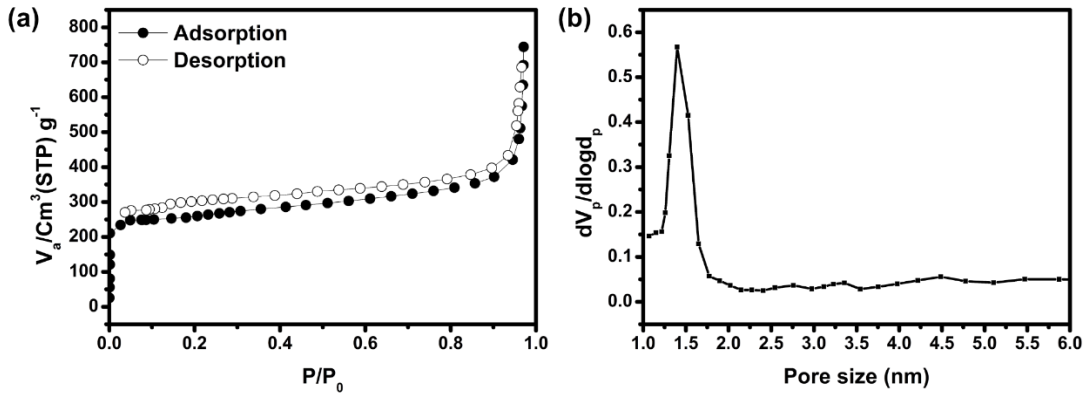

Supplementary Figure 14. (a) Nitrogen adsorption-desorption isotherm and (b) pore size distribution of the hcc-COF powder.

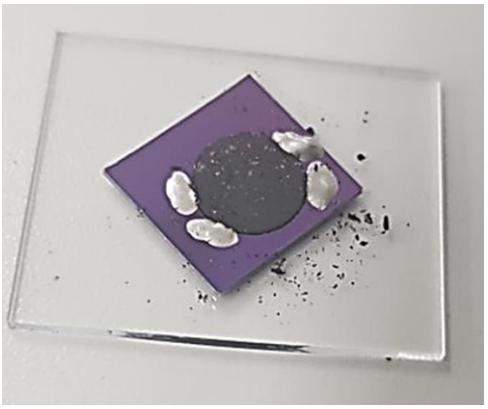

Supplementary Figure 15. Photograph of the hcc-COF pellet device with silver paste electrodes for electrical property measurement.

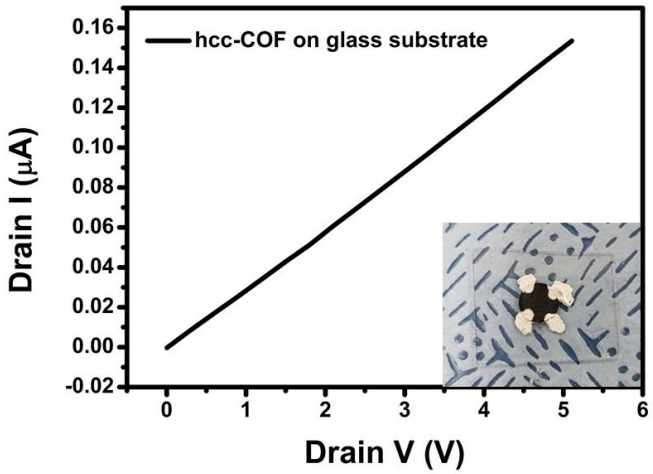

Supplementary Figure 16. I-V characteristic curve of the hcc-COF pellet located on a glass substrate.

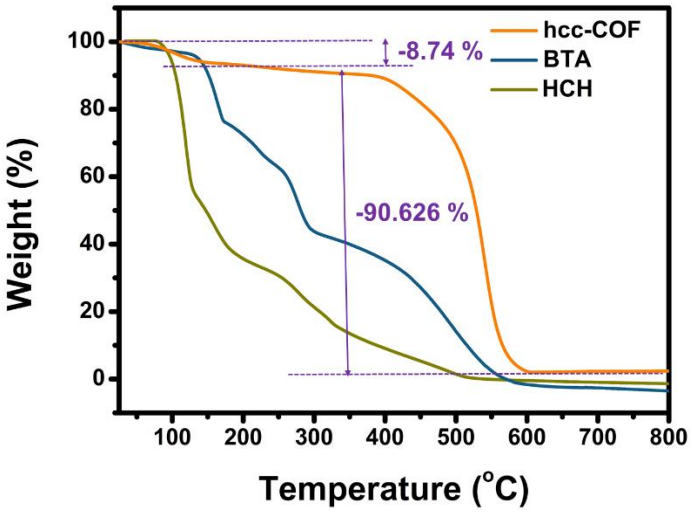

Supplementary Figure 17. TGA data of the hcc-COF (orange) and precursors (BTA (blue) and HCH (green)).

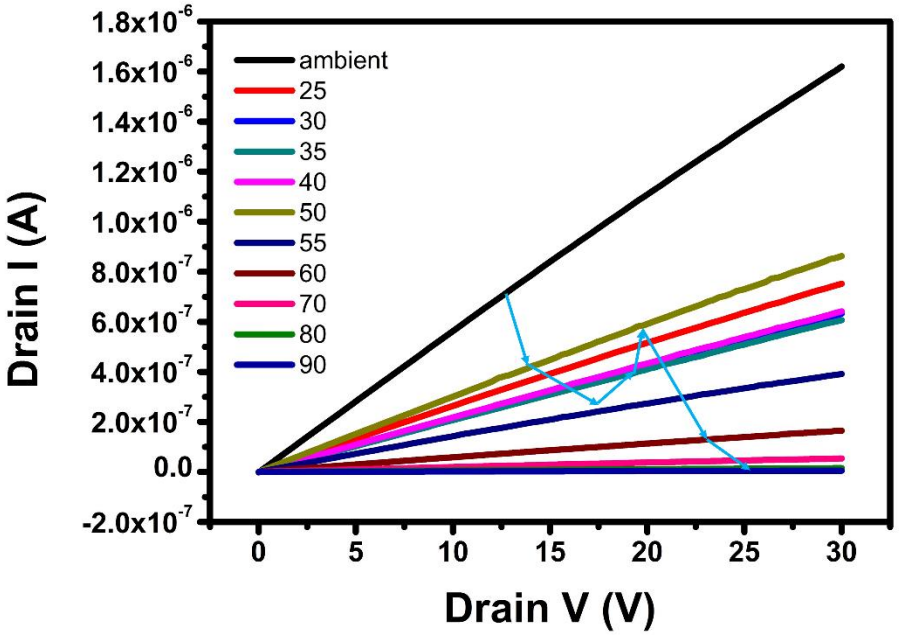

Supplementary Figure 18. Temperature dependent I-V characteristic of hcc-COF in temperature range of ambient to 90 ºC.

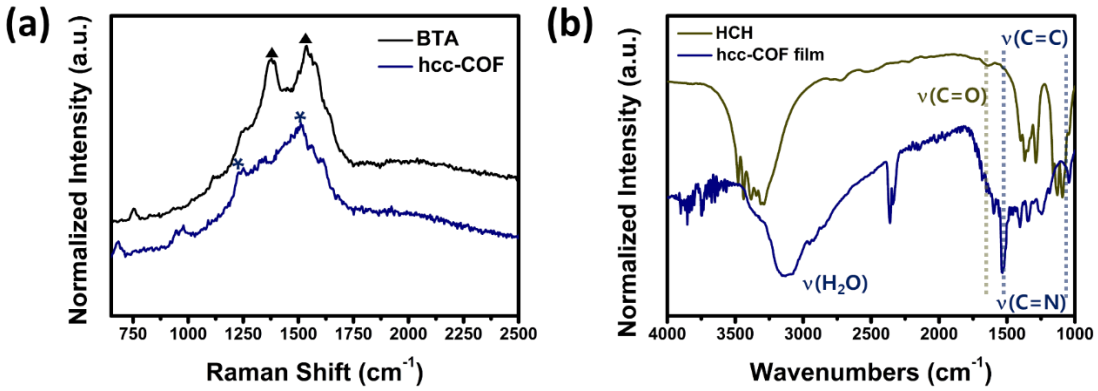

Supplementary Figure 19. (a) Raman and (b) FT-IR spectra of hcc-COF and precursors.

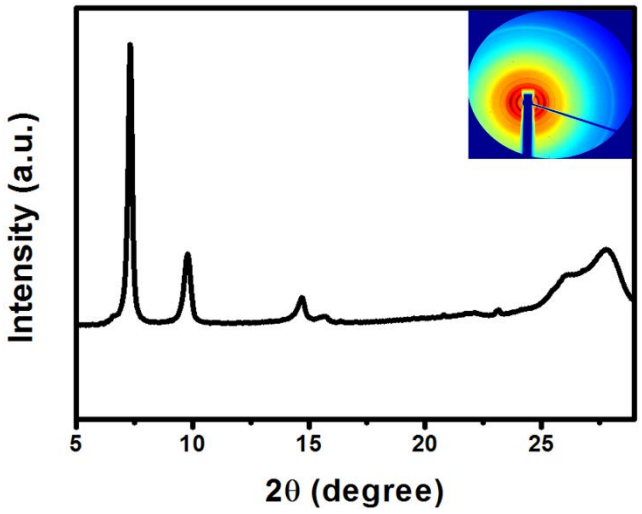

Supplementary Figure 20. WAXD pattern of obtained product synthesized by NMP instead of MeOH, which shows identical diffraction pattern to the previously obtained WAXD pattern.

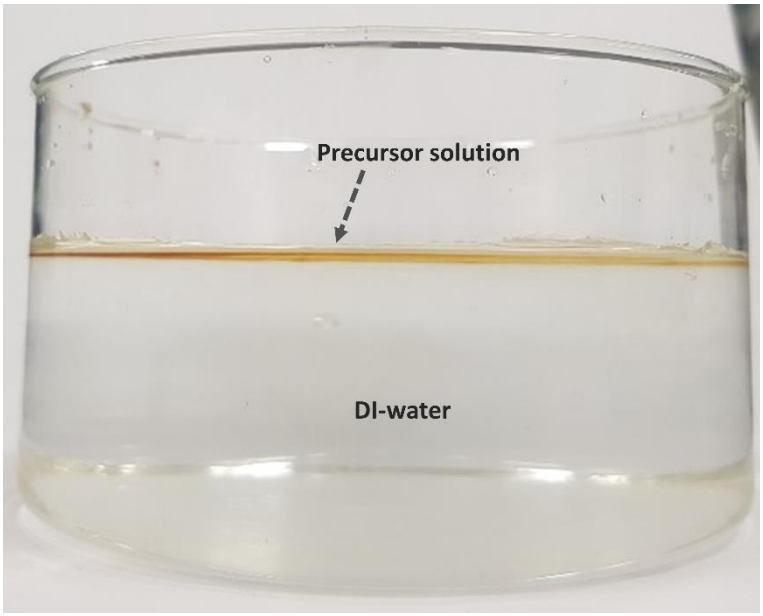

Supplementary Figure 21. Photograph of water surface after deposition of precursor solutions, which is uniformly spread on the water surface.

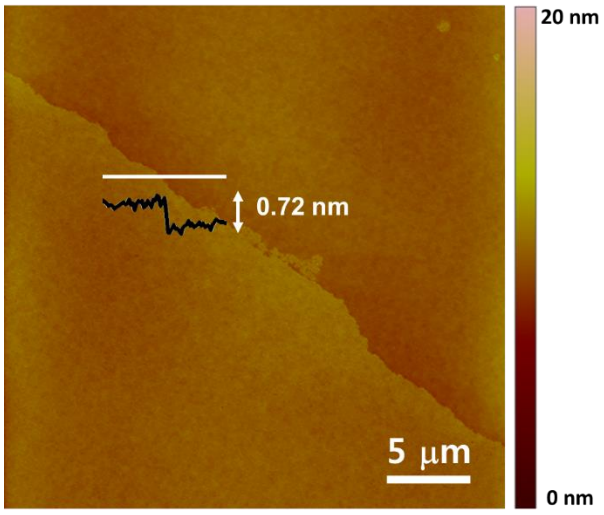

Supplementary Figure 22. AFM image of monolayer hcc-COF film

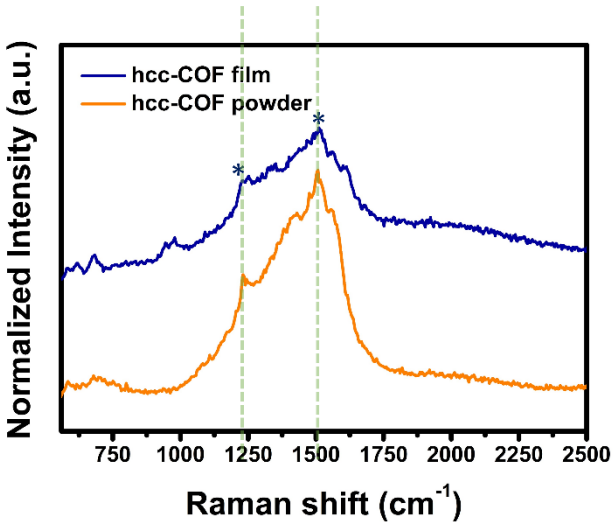

Supplementary Figure 23. Raman spectra of hcc-COF powder (orange) and 2D film (navy). Overall peak shape and two peaks indicated by asterisks (*) of hcc-COF 2D film are well matched with Raman spectrum of hcc-COF powder.

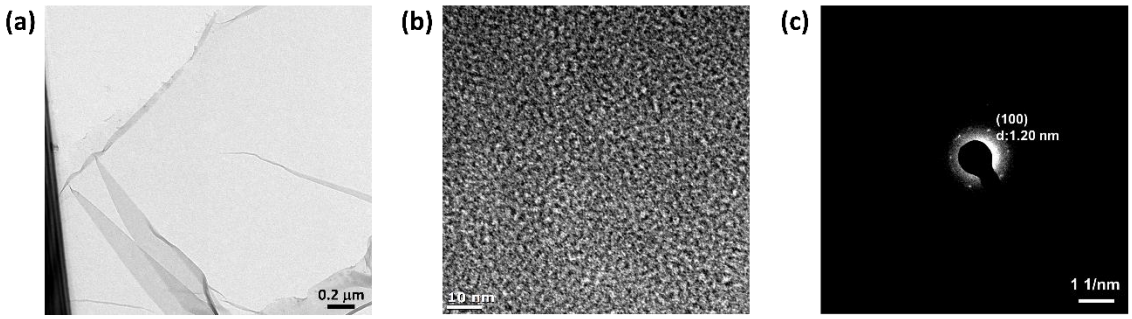

Supplementary Figure 24. TEM images of hcc-COF 2D film at (a) low-magnification and (b) high-magnification (c) ED pattern of the hcc-COF film.

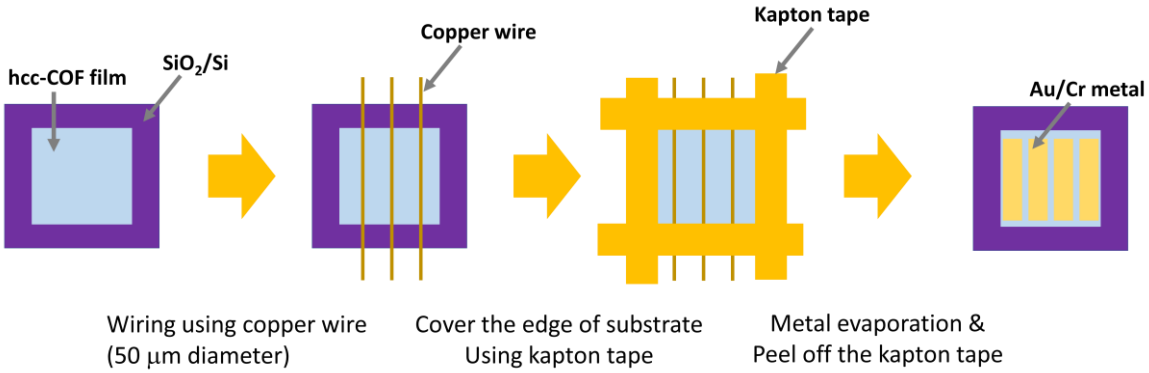

Supplementary Figure 25. Device fabrication of hcc-COF 2D film.

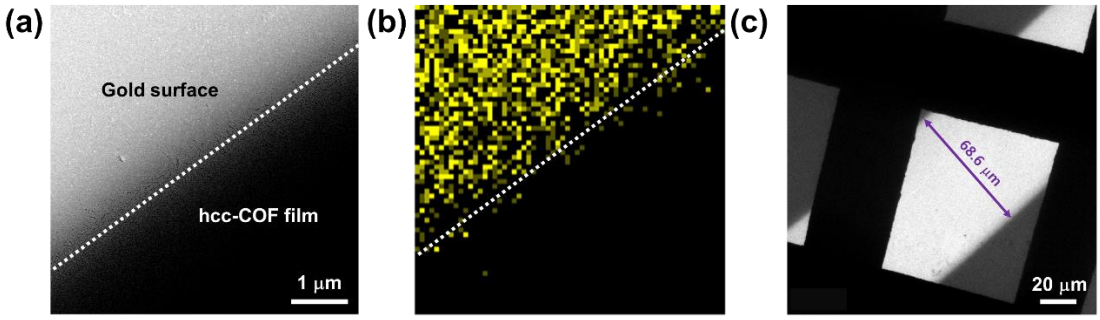

Supplementary Figure 26. (a) Dark-field and (c) low-magnification TEM images of the hcc-COF film device showing clear interface between gold and hcc-COF film (b) EDS mapping image of gold element.

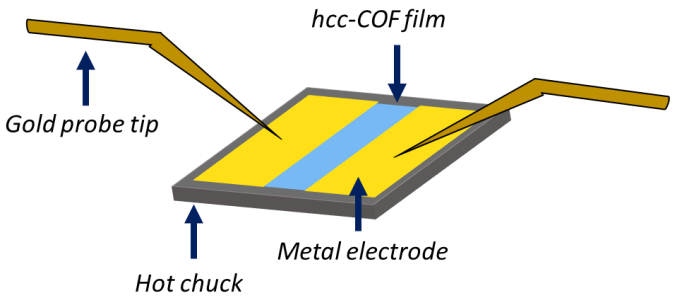

Supplementary Figure 27. Scheme of electrical conductivity measurement of the hcc-COF film device.

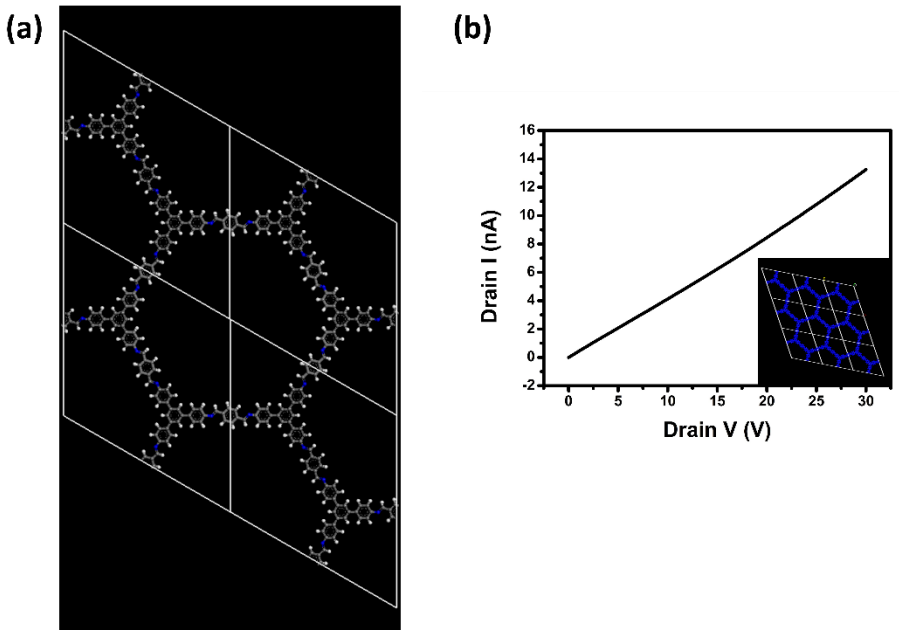

Supplementary Figure 28. (a) Molecular structure of pi-COF (b) I-V characteristic of pi-COF 2D film and inset is iso-surface of electron density.

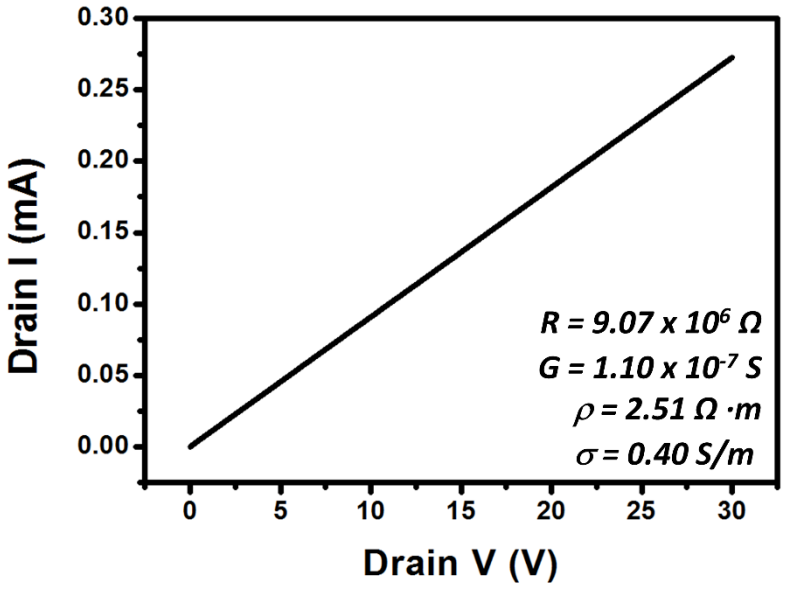

Supplementary Figure 29. I-V characteristic of hcc-COF 2D film.

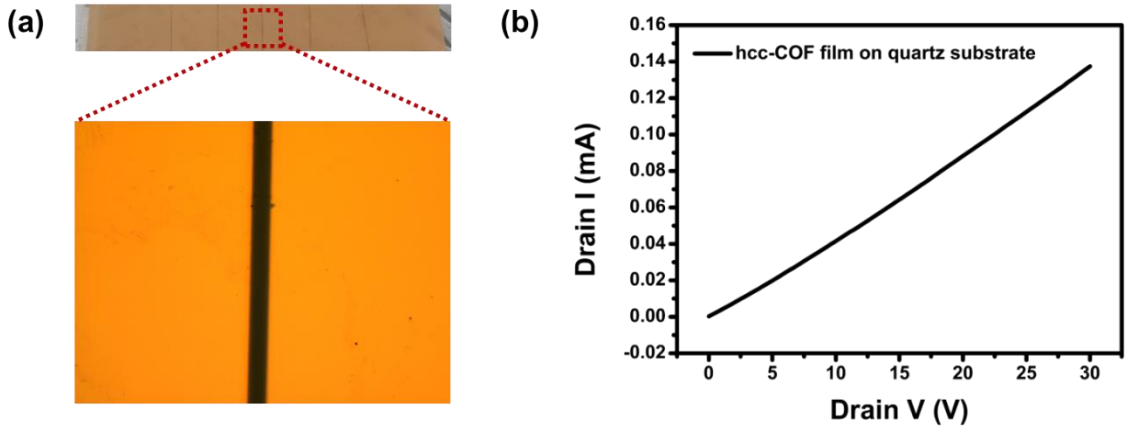

Supplementary Figure 30. (a) The photograph (top), optical microscope images (down) and (b) I-V curve of the resulting hcc-COF film device transferred on a quartz substrate.

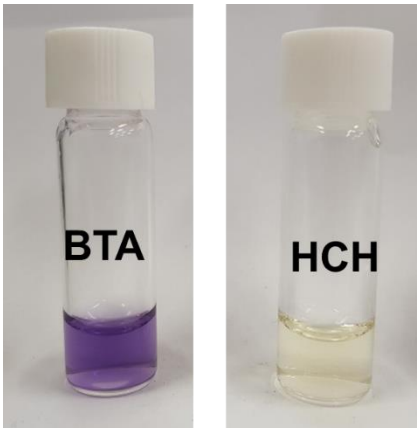

Supplementary Figure 31. BTA and HCH solution solved in DI-water (1 mg/1 mL).

Stacking structure	R_{wp} *(w/background)*	R_{wp} *(w/o background)*
Eclipsed AA	*24.28 %*	*27.22 %*
Serrated AA	*17.05 %*	*16.22 %*
Staggered AB	*24.20 %*	*16.60 %*
Inclined AA	*4.84 %*	*5.12 %*

Supplementary Table 1. Calculated R_{wp} values depending on the model stacking structure of hcc-COF.

(a)

Name	Conductivity
TTF-COF Film[1]	1.2×10^{-4} S/m
sp^2c-COF[2]	6.1×10^{-14} S/m
1-S[3] 1-Se[3] 1-Te[3]	3.7×10^{-10} S/m 8.4×10^{-9} S/m 1.3×10^{-7} S/m
por-COF[4]	4.6×10^{-11} S/m
Aza-CMP[5]	3×10^{-5} S/m

(b)

Name	Conductivity
TCNQ doped TTF-COF Film[1]	0.28 S/m
Iodine doped TTF-COF film[1]	1×10^{-3} S/m
Iodine doped sp^2c-COF[2]	7.1×10^{-2} S/m
Iodine doped por-COF[4]	1.52×10^{-7} S/m

Supplementary Table 2. Electrical conductivity of other reported (a) COFs and (b) doped COFs up to date

Supplementary References

1. Cai, S.L. et al. Tunable electrical conductivity in oriented thin films of tetrathiafulvalene-based covalent organic framework. *Chem. Sci.* **5**, 4693-4700 (2014).

2. Jin, E.Q. et al. Two-dimensional sp^2 carbon-conjugated covalent organic frameworks. *Science* **357**, 673-676 (2017).

3. Duhovic, S. & Dinca, M. Synthesis and Electrical Properties of Covalent Organic Frameworks with Heavy Chalcogens. *Chem. Mater.* **27**, 5487-5490 (2015).

4. Nath, B. et al. A new azodioxy-linked porphyrin-based semiconductive covalent organic framework with I-2 doping-enhanced photoconductivity. *CrystEngComm.* **18**, 4259-4263 (2016).

5. Briega-Martos, V. et al. An Aza-Fused π-Conjugated Microporous Framework Catalyzes the Production of Hydrogen Peroxide. *ACS Catal.* **7**, 1015-1024 (2017).